Adaptive methods for dynamical micromagnetics

Ľubomír Baňas[1]*

Ghent university, Ghent, Belgium l.banas@imperial.ac.uk

Summary. We propose a space-time adaptive algorithm for two iterative numerical methods for the solution of nonlinear time depended Landau-Lifshitz-Gilbert equation of micromagnetism. The first method is derived from implicit backward Euler time discretisation, the second method is based on midpoint rule. The space discretisation is done by linear finite elements. The resulting nonlinear systems are solved by an iterative fixed-point technique. The performance of the proposed adaptive strategy is demonstrated by numerical experiments.

1 Introduction

The Landau-Lifshitz-Gilbert (LLG) equation plays an important role in applications which require simulation of nonlinear magnetic behaviour on microscale such as, e.g., magnetic recording. The time dependent LLG equation takes the form [13]

$$\partial_t \boldsymbol{m} = \boldsymbol{h}_T \times \boldsymbol{m} + \alpha \boldsymbol{m} \times (\boldsymbol{h}_T \times \boldsymbol{m}) \quad \text{in} \quad \Omega \times (0,T) \tag{1}$$

where $\boldsymbol{m} \in \mathbb{R}^3$ is the magnetisation vector, Ω is a bounded domain with sufficiently smooth boundary; α is so called damping constant. The total field $\boldsymbol{h}_T$ from (1) can consist of several contributions, here we take

$$\boldsymbol{h}_T = \Delta \boldsymbol{m} + \boldsymbol{h},$$

where $\Delta \boldsymbol{m}$ is exchange field. The magnetic field $\boldsymbol{h}$ can be obtained from the Maxwell's equations, for simplicity we treat it as a known vector field throughout the rest of the paper.

We consider a homogeneous Neumann boundary condition at the boundary Γ i.e.

$$\frac{\partial \boldsymbol{m}}{\partial \boldsymbol{\nu}} = \boldsymbol{0} \quad \text{on} \quad \partial\Omega.$$

* Currently with: Imperial College, London, UK

and initial condition $\boldsymbol{m}(0) = \boldsymbol{m}_0$ in Ω.

A scalar multiplication of (1) by $\boldsymbol{m}$ gives

$$\partial_t \boldsymbol{m} \cdot \boldsymbol{m} = \frac{1}{2}\partial_t |\boldsymbol{m}|^2 = 0. \tag{2}$$

This implies conservation of magnitude of magnetisation $|\boldsymbol{m}(t)| = |\boldsymbol{m}_0| = 1$, which is an important conservation property of the LLG equation.

By combining (2) with the standard vector cross-product formula

$$\boldsymbol{a} \times (\boldsymbol{b} \times \boldsymbol{c}) = (\boldsymbol{a} \cdot \boldsymbol{c})\boldsymbol{b} - (\boldsymbol{a} \cdot \boldsymbol{b})\boldsymbol{c},$$

we obtain the following identity

$$\boldsymbol{m} \times (\boldsymbol{m} \times \Delta \boldsymbol{m}) = -\Delta \boldsymbol{m} - |\nabla \boldsymbol{m}|^2 \boldsymbol{m}.$$

From this, we see, that for sufficiently smooth solutions, (1) is equivalent to

$$\begin{aligned} \partial_t \boldsymbol{m} - \alpha \Delta \boldsymbol{m} = \alpha |\nabla \boldsymbol{m}|^2 \boldsymbol{m} + \Delta \boldsymbol{m} \times \boldsymbol{m} \\ + \alpha(\boldsymbol{h} - (\boldsymbol{h} \cdot \boldsymbol{m})\boldsymbol{m}) + \boldsymbol{h} \times \boldsymbol{m}. \end{aligned} \tag{3}$$

This implies a close relation of LLG equation to the harmonic maps equation.

Another equivalent formulation of (1), the so-called Gilbert form of the LLG equation ([10]) is given by

$$\boldsymbol{m}_t - \alpha \boldsymbol{m} \times \boldsymbol{m}_t = (1 + \alpha^2)\boldsymbol{m} \times \boldsymbol{h}_T. \tag{4}$$

The numerical solution of (1) will be based on formulations (3) and (4).

2 Numerical methods

We define the following spaces of vector functions: $\mathbf{L}_2(\Omega) = (L_2(\Omega))^3$, $\mathbf{H}^1(\Omega) = (H^1(\Omega))^3$, where $L_2(\Omega)$ and $H^1(\Omega)$ are the usual function spaces. We denote the $\mathbf{L}_2(\Omega)$-inner product by $(\boldsymbol{a}, \boldsymbol{b}) = \int_\Omega (\boldsymbol{a} \cdot \boldsymbol{b})$. The discrete inner product is defined as $(\boldsymbol{a}, \boldsymbol{b})_h = \int_\Omega \mathcal{I}^h(\boldsymbol{a} \cdot \boldsymbol{b})$ where $\mathcal{I}^h$ is the usual interpolation operator. The notation $\|\cdot\|$ stands for the $\mathbf{L}_2$ norm and $\|\cdot\|_1$ is $\mathbf{H}^1$ norm.

We divide the time interval $(0, T)$ into subintervals (t_i, t_{i+1}), $i = 0, \ldots, n$ with variable time step size $\tau_{i+1} = t_{i+1} - t_i$. We denote by $\mathcal{T}^i$ a quasi-uniform partition of Ω into simplices (see [7]) on time level i. The triangulation $\mathcal{T}^i$ is obtained from $\mathcal{T}^{i-1}$ by refinement or coarsening. Given a triangle $K \in \mathcal{T}^i$, h_K stands for its diameter. We also denote by $\mathcal{E}^i$ the set of all edges e from $\mathcal{T}^i$, h_e denotes the size of $e \subset E^i$ and by a_j, $j = 1, \ldots, N_i$ the set of all vertices from $\mathcal{T}_i$. The space $\mathbf{V}_i^h \subset \mathbf{H}^1$ is the space of finite element functions that are piecewise linear on $\mathcal{T}^i$.

2.1 Backward Euler projection scheme

The implicit backward Euler time discretisation method for the LLG equation is derived from the formulation (3). It is a known fact, that the backward Euler discretisation violates (2), therefore a projection step is needed to enforce the constraint explicitely in the numerical approximation. The continuous variational formulation of (3) reads as follows

$$(\boldsymbol{m}_t, \boldsymbol{\psi}) + \alpha(\nabla \boldsymbol{m}, \nabla \boldsymbol{\psi}) = \alpha(|\nabla \boldsymbol{m}|^2 \boldsymbol{m}, \boldsymbol{\psi}) - (\boldsymbol{m} \times \nabla \boldsymbol{m}, \nabla \boldsymbol{\psi}) \quad \forall \boldsymbol{\psi} \in \mathbf{H}^1(\Omega).$$

Then the implicit backward Euler projection scheme based on the above variational formulation consists of two steps

- solve

$$\begin{aligned}\left(\frac{\boldsymbol{m}^h_{i+1} - \boldsymbol{m}^{h,*}_i}{\tau_{i+1}}, \boldsymbol{v}\right)_h + \alpha(\nabla \boldsymbol{m}^h_{i+1}, \nabla \boldsymbol{v}) = {} & \alpha(|\nabla \boldsymbol{m}^h_{i+1}|^2 \boldsymbol{m}^h_{i+1}, \boldsymbol{v})_h \\ & -(\boldsymbol{m}^h_{i+1} \times \nabla \boldsymbol{m}^h_{i+1}, \nabla \boldsymbol{v}) \\ & +\alpha(\boldsymbol{h}^h_{i+1} - (\boldsymbol{h}^h_{i+1} \cdot \boldsymbol{m}^h_{i+1})\boldsymbol{m}^h_{i+1}) \\ & +\boldsymbol{h}^h_{i+1} \times \boldsymbol{m}^h_{i+1} \\ & \forall \boldsymbol{v} \in \mathbf{V}^h_{i+1}(\Omega).\end{aligned} \tag{5}$$

- project the solution

$$\boldsymbol{m}^{h,*}_{i+1}(\boldsymbol{a}_j) = \frac{\boldsymbol{m}^h_{i+1}(\boldsymbol{a}_j)}{|\boldsymbol{m}^h_{i+1}(\boldsymbol{a}_j)|} \quad j = 1, \ldots, k.$$

The discrete system (5) is nonlinear. We solve the system by a fixed point technique. Starting with $k = 0$, $\boldsymbol{m}^h_{i,0} = \boldsymbol{m}^h_i$ we compute

$$\begin{aligned}\left(\frac{\boldsymbol{m}^h_{i+1,k+1} - \boldsymbol{m}^{h,*}_i}{\tau_{i+1}}, \boldsymbol{v}\right)_h + \alpha(\nabla \boldsymbol{m}^h_{i+1,k+1}, \nabla \boldsymbol{v}) = {} & \alpha(|\nabla \boldsymbol{m}^h_{i+1,k}|^2 \boldsymbol{m}^h_{i+1,k+1}, \boldsymbol{v})_h \\ & -(\boldsymbol{m}^h_{i+1,k} \times \nabla \boldsymbol{m}^h_{i+1,k+1}, \nabla \boldsymbol{v}) \\ & +\alpha(\boldsymbol{h}^h_{i+1} - (\boldsymbol{h}^h_{i+1} \cdot \boldsymbol{m}^h_{i+1,k})\boldsymbol{m}^h_{i+1,k+1}) \\ & +\boldsymbol{h}^h_{i+1} \times \boldsymbol{m}^h_{i+1,k+1} \\ & \forall \boldsymbol{v} \in \mathbf{V}^h_{i+1}(\Omega).\end{aligned} \tag{6}$$

until the difference

$$\|\boldsymbol{m}^h_{i+1,k+1} - \boldsymbol{m}^h_{i+1,k}\|_h < TOL$$

where TOL is a sufficiently small prescribed tolerance.

2.2 Midpoint rule

We introduce some additional notation. The midpoint values of the numerical solution are denoted by $\boldsymbol{m}^h_{i+1/2} = \frac{1}{2}(\boldsymbol{m}^h_{i+1} + \boldsymbol{m}^h_i)$, the discrete Laplacian $\Delta_h : \mathbf{H}^1(\Omega) \to \mathbf{V}^h$ is represented by the formula

$$(\Delta_h \boldsymbol{u}, \boldsymbol{v})_h = (\nabla \boldsymbol{u}, \nabla \boldsymbol{v}) \quad \forall \boldsymbol{v} \in \mathbf{V}^h_{i+1}(\Omega).$$

The midpoint rule in the context of micromagnetism was studied in a number of works, e.g., [14], [18], [3]. We will use the formulation from [3] which reads as

$$\begin{aligned}&\left(\tfrac{\boldsymbol{m}^h_{i+1}-\boldsymbol{m}^h_i}{\tau_{i+1}}, \boldsymbol{v}\right)_h + \alpha\left(\boldsymbol{m}^h_i \times \tfrac{\boldsymbol{m}^h_{i+1}-\boldsymbol{m}^h_i}{\tau_{i+1}}, \boldsymbol{v}\right)_h \\ &= \\ &(1+\alpha^2)(\boldsymbol{m}^h_{i+1/2} \times \Delta_h \boldsymbol{m}^h_{i+1/2}, \boldsymbol{v})_h \qquad \forall \boldsymbol{v} \in \mathbf{V}^h_{i+1}(\Omega).\end{aligned} \tag{7}$$

By taking $\boldsymbol{v} = (\boldsymbol{m}^h_{i+1} + \boldsymbol{m}^h_i)\boldsymbol{\varphi}^j$ ($\boldsymbol{\varphi}^j \in \mathbf{V}^h_i$ is a base function which satisfies $\boldsymbol{\varphi}^j(\boldsymbol{a}_j) = 1$) in (7) we immediately see that $\boldsymbol{m}^h_{i+1}(\boldsymbol{a}_j)| = 1$.

Similarly as in the previous case we solve the nonlinear system (7) by a fixed-point technique (cf. [3]). We compute

$$\begin{aligned}&\left(\frac{\boldsymbol{m}^h_{i+1,k+1} - \boldsymbol{m}^h_i}{\tau_{i+1}}, \boldsymbol{v}\right)_h + \alpha\left(\boldsymbol{m}^h_i \times \boldsymbol{m}^h_{i+1,k+1}, \boldsymbol{v}\right)_h \\ &-\frac{(1+\alpha^2)}{4}(\boldsymbol{m}^h_{i+1,k+1} \times \Delta_h \boldsymbol{m}^h_{i+1,k}, \boldsymbol{v})_h - \frac{(1+\alpha^2)}{4}(\boldsymbol{m}^h_{i+1,k+1} \times \Delta_h \boldsymbol{m}^h_i, \boldsymbol{v})_h \\ &-\frac{(1+\alpha^2)}{4}(\boldsymbol{m}^h_i \times \Delta_h \boldsymbol{m}^h_{i+1,k+1}, \boldsymbol{v})_h \\ &= \\ &\frac{(1+\alpha^2)}{4}(\boldsymbol{m}^h_i \times \Delta_h \boldsymbol{m}^h_i, \boldsymbol{v})_h,\end{aligned} \tag{8}$$

until

$$\|\boldsymbol{m}^h_{i+1,k+1} - \boldsymbol{m}^h_{i+1,k}\|_h < TOL,$$

where TOL is a prescribed tolerance.

3 Adaptive algorithm

Our adaptive algorithm makes use of the local error indicators μ^τ_{i+1} and $\mu^h_{K,i+1}$ for the time step control and mesh refinement, respectively (see e.g., [8],[16], [6], [9], [12],[15], [21] for related works). For adaptive techniques in micromagnetism see, e.g., [1], [17], [11], [20].

The local error indicators can be obtained from the a posteriori error estimates (cf. [5]) and take the following form

$$\mu^\tau_{i+1} = \|\boldsymbol{m}^h_{i+1} - \boldsymbol{m}^h_i\|_1^2 + \int_{t_i}^{t_{i+1}} \|(\boldsymbol{h} - \boldsymbol{h}_{i+1})\|^2, .$$

$$\begin{aligned}\mu^h_{K,i+1} = &\sum_{e \subset K} h_e \| \left[\nabla \boldsymbol{m}^h_{i+1} \cdot \boldsymbol{\nu}_e\right]_e \|^2_{L_2(e)} + \|h_K |\nabla \boldsymbol{m}^h_{i+1}|^2 \boldsymbol{m}^h_{i+1}\|^2_{L_2(K)} \\ &+ \left\| h_K \tfrac{\boldsymbol{m}^h_{i+1}-\boldsymbol{m}^h_i}{\tau_{i+1}} \right\|^2_{L_2(K)} + \|h_K(\boldsymbol{h}_{i+1} - \boldsymbol{h}^h_{i+1})\|^2_{L_2(K)}\end{aligned}$$

For a given tolerance TOL start with $\mathcal{T}_0$, τ_0, $\boldsymbol{m}^h_0$.

1. until $t_{i+1} < T$ set $\tau_{i+1} = \tau_i$, $\mathcal{T}_{i+1} = \mathcal{T}_i$;

2. set $t_{i+1} = t_i + \tau_{i+1}$ and compute the discrete solution by (6) or (8), if $\mu^{\tau}_{i+1} \leq \varepsilon^r_\tau TOL$ proceed with the space refinement step 3, else decrease τ_{i+1} step and repeat step 1;

3. for all $K \in \mathcal{T}_{i+1}$, if $\mu^h_{K,i+1} > \varepsilon^r_h TOL/N_{i+1}$ mark K for refinement, if $\mu^h_{K,i+1} < \varepsilon^c_h TOL/N_{i+1}$ mark K for coarsening;

4. refine/coarsen mesh and compute new solution, if , $\mu^{\tau}_{i+1} \leq \varepsilon^c_\tau TOL$ increase τ_{i+1} and go to step 2 (this can be repeated several times, otherwise we proceed to the next time step with, i.e. we go to step 1).

The constants ε^r_τ, ε^c_h are chosen (e.g. 0.5, 0.5), N_{i+1} is the number of elements from $\mathcal{T}_{i+1}$.

4 Numerical experiment

In this numerical example we will apply our adaptive strategy to a problem from [2], [3]. There this problem has been studied on uniform meshes. The problem is computed in domain $\Omega = (0,1) \times (0,1)$ with $\boldsymbol{h} \equiv \mathbf{0}$ and initial data ($\boldsymbol{x} = (x_1 - 0.5, x_2 - 0.5)$)

$$\boldsymbol{m}_0(\boldsymbol{x}) = \begin{cases} (2\boldsymbol{x}A, A^2 - |\boldsymbol{x}|^2)/(A^2 + |\boldsymbol{x}|^2) & \boldsymbol{x} \leq 0.5 \\ (0, 0, -1) & \boldsymbol{x} \geq 0.5. \end{cases}$$

where $A = (1 - 2|\boldsymbol{x}|)^4/16$. The initial data is chosen in such a way that after a finite time a singularity (i.e. $\nabla \boldsymbol{m} \notin \mathbf{L}_\infty(\Omega)$) starts to form in the middle of the domain. We studied the problem on time interval $t \in (0, 0.31)$.

The initial mesh and mesh at final time are depicted in Figures 1 (49563 unknowns) and Figure 2 (34395 unknowns for midpoint method and 34491 unknowns for backward-Euler method). For this particular choice of parameters in adaptive algorithm, the meshes at the final time were graphically indistinguishable for both methods. The three components of the magnetisation near the time $t = 0.31$ are depicted in Figures 3-5. Again, the results were graphically identical for both methods. It is clear from the results that the adaptive algorithm correctly detect the position of the singularity and increases the efficiency of the computation.

The time step size for both methods varied from $\mathcal{O}(1^{-5})$ to $\mathcal{O}(1^{-7})$. In [3] the authors need $\tau = \mathcal{O}(h^2)$ for the convergence of (8) on uniform meshes. With our adaptive strategy we attained numerical convergence of the fixed-point iterations (8) while using larger time steps for midpoint method. The time step sizes for the midpoint method were comparable to those used with the backward Euler method, which is robust with respect to mesh refinement (cf. [19],[4]). The evolutions of number of unknowns (i.e. vertices of the mesh) during the computation can be found in figures (6) and (7).

Although, the used adaptive algorithm was originally developed for backward-Euler method (see [5]), the presented numerical results indicate, that it can be successfully used with midpoint method. Moreover, the behaviour of both adaptive methods (e.g. mesh evolution and topology, time stepping) was very similar in our experiments.

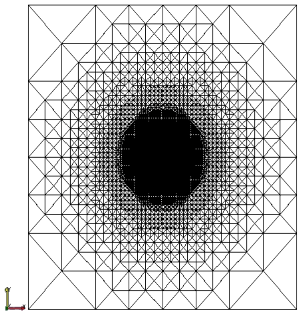

Fig. 1. Initial Mesh

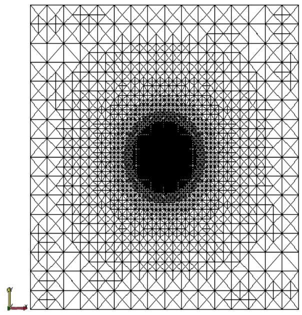

Fig. 2. Mesh at final time

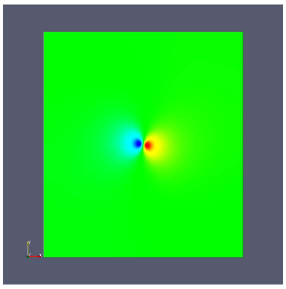

Fig. 3. x-component of $\boldsymbol{m}$

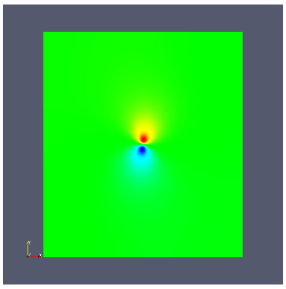

Fig. 4. y-component of $\boldsymbol{m}$

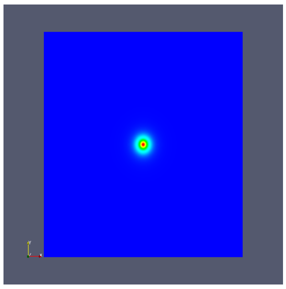

Fig. 5. z-component of $\boldsymbol{m}$

Acknowledgements

The author would like to acknowledge the support of the IUAP project of the Ghent University and the EPSRC grant of the Imperial College.

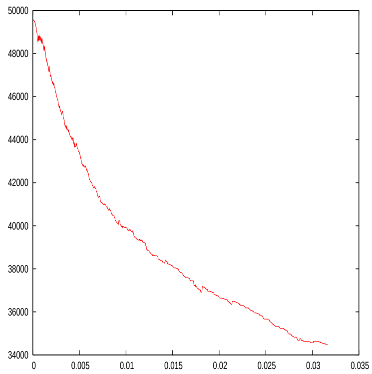

Fig. 6. Degrees of freedom for backward-Euler method

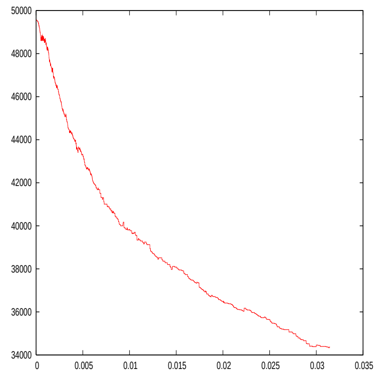

Fig. 7. Degrees of freedom for midpoint method

References

1. Bagnérés-Viallix, A., Baras, P., Albertini, J.B.: 2D and 3D calculations of micromagnetic wall structures using finite elements. IEEE Trans. Magn., **27**, 3819–3822 (1991)
2. Bartels, S., Ko, J., Prohl., A.: Numerical approximation of the Landau-Lifshitz-Gilbert equation and finite time blow-up of weak solutions. preprint, http://www.fim.math.ethz.ch/preprints, (2005)
3. Bartels, S., Prohl, A.: Convergence of an implicit finite element method for the Landau-Lifshitz-Gilbert eqauation. preprint, http://www.fim.math.ethz.ch/preprints, (2005)
4. Baňas, Ľ.: Numerical methods for the Landau-Lifshitz-Gilbert equation. In: Li, Z., Vulkov, L., Wasniewski, J. (eds) Numerical Analysis and Its Applications: Third International Conference, NAA 2004, Rousse, Bulgaria, June 29-July 3, 2004, Revised Selected Papers. Lecture Notes in Computer Science, **3401**, Springer (2005)
5. Baňas, Ľ.: On dynamical micromagnetism with magnetostriction. PhD thesis, Ghent University, Ghent (2005)
6. Chen, Z., Dai., S.: Adaptive galerkin methods with error control for a dynamical Ginzburg-Landau model in superconductivity. SIAM J. Numer. Anal., **38**, 1961–1985 (2001)
7. Ciarlet., P.G.: The finite element method for elliptic problems. North-Holland, Amsterdam (1978)
8. Eriksson, K., Johnson., C.: Adaptive finite element methods for parabolic problems I: A linear model problem. SIAM J. Numer. Anal., **28**, 43–77 (1991)
9. Eriksson, K., Johnson, C.: Adaptive finite element methods for parabolic problems IV: Nonlinear problems. SIAM J. Numer. Anal., **32**, 1729–1749 (1995)
10. Gilbert., T.L.: A Lagrangian formulation of gyromagnetic equation of the magnetic field. Phys. Rev., **100:1243**, (1955)
11. Hertel, R., Kronmüller, H.: Adaptive finite element mesh refinement techniques in three-dimensional micromagnetic modeling. IEEE Trans. Magn., **34**, 3922–3930 (1998)

12. Ivarsson, J.: A posteriori error analysis in $L_2(L_2)$ and $L_2(H^1)$ of the discontinuous Galerkin method for the time-dependent Ginzburg-Landau equations. preprint, (2001)
13. Landau, L.D., Lifshitz, E.M.: Electrodynamics of continuous media. Translated from the Russian by J.B. Sykes and J.S. Bell. Pergamon Press, Oxford-London-New York-Paris (1960)
14. Monk, P.B., Vacus, O.: Accurate discretization of a nonlinear micromagnetic problem. Comput. Methods Appl. Mech. Eng., **190**, 5243–5269 (2001)
15. Nochetto, R.H., Schmidt, A., Verdi, C.: A posteriori error estimation and adaptivity for degenerate parabolic problems. SIAM J. Numer. Anal., **69**, 1–24 (2000)
16. Picasso., M.: Adaptive finite elements for a linear parabolic problem. Comput. Meth. Appl. Mech. Eng., **167**, 223–237 (1998)
17. Scholz, W., Schrefl, T., Fidler, J.: Mesh refinement in Fe-micromagnetics for multi-domain $Nd_2Fe_{14}B$ particles. J. Magn. Magn. Mater., **196-197**, 933–934 (1999)
18. Serpico, C., Mayergoyz, I.D., Bertotti, G.: Numerical technique for integration of the Landau-Lifshitz equation. J. Appl. Phys., **89**, 6991–6993 (2001).
19. Suess, D., Tsiantos, V., Schrefl, T., Fidler, J., Scholz, W., Forster, R., Dittrich, H., Miles J.J.: Time resolved micromagnetics using a preconditioned time integration method. J. Magn. Magn. Mater., **248**, 298–311 (2002)
20. Tako, K.M., Schrefl, T., Wongsam, M.A., Chantrell, R.W.: Finite element micromagnetic simulations with adaptive mesh refinement. J. Appl. Phys., **81**, 4082–4084 (1997)
21. Verfürth, R.: A posteriori error estimates for nonlinear problems. $L^r(0,t;L^\rho(\Omega))$-error estimates for finite element discretizations of parabolic equations. Math. Comp., **67**, 1335–1360 (1998)